

# Errorless Robust JPEG Steganography using Outputs of JPEG Coders

Jan Butora, Pauline Puteaux and Patrick Bas

**Abstract**—Robust steganography is a technique of hiding secret messages in images so that the message can be recovered after additional image processing. One of the most popular processing operations is JPEG recompression. Unfortunately, most of today’s steganographic methods addressing this issue only provide a probabilistic guarantee of recovering the secret and are consequently not errorless. That is unacceptable since even a single unexpected change can make the whole message unreadable if it is encrypted. We propose to create a robust set of DCT coefficients by inspecting their behavior during recompression, which requires access to the targeted JPEG compressor. This is done by dividing the DCT coefficients into 64 non-overlapping lattices because one embedding change can potentially affect many other coefficients from the same DCT block during recompression. The robustness is then combined with standard steganographic costs creating a lattice embedding scheme robust against JPEG recompression. Through experiments, we show that the size of the robust set and the scheme’s security depends on the ordering of lattices during embedding. We verify the validity of the proposed method with three typical JPEG compressors and benchmark its security for various embedding payloads, three different ways of ordering the lattices, and a range of Quality Factors. Finally, this method is errorless by construction, meaning the embedded message will always be readable.

**Index Terms**—robust steganography, recompression, lattice embedding, JPEG

## I. INTRODUCTION

With the wide usage of social networks and sharing platforms, the classical setup of steganography, which implies a lossless channel between Alice (the steganographer who embeds a payload) and Bob (the steganographer who decodes a payload), is meaningless in a lot of practical scenarios. This is due to the fact that the transmission channel involves a transcoding of the stego content (a JPEG recompression, for example) which can be seen as a noisy channel between Alice and Bob. In such a case, the errorless decoding of the payload is not possible anymore if Alice uses classical embedding schemes designed for lossless transmission (*e.g.* in the JPEG domain with the use of J-Uniward [1], UERD [2], J-Mipod [3], ...). Moreover, note that if the embedded payload is encrypted – which is usually the case for security reasons – decoding the embedded message is not possible as soon as one bit of the payload is changed.

### A. Prior Works on Robust Steganography

The domain of robust steganography aims at keeping the main constraint of steganography (*i.e.* to embed an undetectable payload) but also adds the constraint of robustness, which can be defined as minimizing the bit error rate on the decoded payload after a lossy transmission channel. Note

that this second constraint (robustness) is very similar to the one defined in watermarking. For this reason, secure watermarking [4] could hypothetically be considered as an option to embed robust and undetectable payload [5]. However, the proposed schemes in the watermarking literature never considered either steganalysis to benchmark undetectability or large embedding rates. In watermarking, the payload characterizes an identifier of several dozens of bits, not a message of several kilobits.

In [6], Cleaves and Ker both study the impact of lossy transmission combined with syndrome trellis code (STC) [7]. They show that the STC replicates the errors associated with the channel on the decoded payload. They propose to use a dual-STC scheme combined with Reed-Solomon (RS) Error Correcting Codes (ECC) to reduce the error rate while minimizing the embedding distortion. This scheme is, however, not benchmarked w.r.t. steganalysis.

Zhang *et al.* proposed to mix a watermarking scheme [8] based on the modifications of DCT coefficients [9] and a steganographic scheme [1] to favor embedding on coefficients which are both robust and secure by weighting the cost related to J-UNIWARD. Unfortunately, the proposed scheme is very detectable (*e.g.*  $P_E = 5\%$  at quality factor QF = 75 and 0.1 bpnzAC). The payload also needs to be protected using RS-ECC, and the error rate is still essential for large QF (19% at QF = 95).

In [10], Qiao *et al.* propose to select robust cover elements, which are defined as robust because they are not equal to zero after double compression. Unfortunately, this scheme suffers from at least two drawbacks: 1) Alice has to transmit the set of robust elements to Bob as side information, and 2) the payload is still subject to errors, and the detectability is, by a large amount, more important than the non-robust scheme.

Tao *et al.* propose the idea to generate an *intermediate image* after embedding by the mean of “coefficient adjustment” [11]. This image is a modified version of the stego image, and the modifications are computed to cancel the modifications due to an ideal JPEG coding scheme. A similar idea to invert the JPEG compression scheme was developed by Lu *et al.* by combining coefficient adjustment with an auto-encoder predicting the input image [12]. In both cases, the changes made to the intermediate image increase the detectability of the modified stego image. The practical implementation of finding a perfect intermediate image is also questioned in [12] due to convergence issues. The authors adopt another strategy using the auto-encoder, but it cannot cancel all the modifications due to coding.

The last line of research on this topic is the scheme proposed by Zhao *et al.* [13]. Successive compressions of the

cover image are used to reduce the number of changes after embedding and compression. This method is effective but has the disadvantage of generating (recompressed) cover images that are different from natural ones, hence more detectable. The proposed scheme also uses BCH-ECC to decrease the error rate after embedding.

It is important to note that, due to the practical context of steganography, the scheme's robustness has to be extremely high, as only one erroneous bit can jeopardize the whole transmission. Errorless steganographic schemes are consequently recommended. Regarding robustness to image scaling, several works address this issue for different downsampling kernels, such as the nearest neighbor kernel or the bilinear kernel, where only pixels that are respectively preserved (see Zhang *et al.* [14]), or contribute the most (see Zhu *et al.* [15]), are modified. To the best of our knowledge, errorless robust JPEG steganography has not been investigated before.

## B. Outline of the Paper

This paper proposes an errorless steganographic scheme in the JPEG domain robust to JPEG recompression. Section II presents both the security setup (*i.e.* the knowledge of the embedder) and the coding setup (*i.e.* the JPEG coding process). Section III details an algorithm proposed to use the output of JPEG coders to extract a set of robust coefficients according to a specific scanning strategy. Section IV presents the embedding and decoding algorithms together with a strategy to spread the payload into 64 lattices. Section V presents results on the detectability of the proposed scheme and compares it with naive embedding. A robustness analysis is also proposed when JPEG coding uses rate-optimization strategies.

## II. CONSIDERED SETUPS

### A. Notations

A bold capital letter is considered as a matrix, and a lowercase letter denotes a coefficient.  $(i, j)$  denotes the pixels or coefficients coordinates  $i$  and  $j$ .

### B. Security Setup

We first mention the security setup considered in this study, which is also illustrated on the top diagram of Fig. 1. Alice, the embedder, sends a stego image, denoted  $S_1$ , on a platform that compresses  $S_1$  into  $S_2$  using a JPEG coder. Bob, the receiver, downloads the image from the platform and tries to decode the payload. Because we assume that Alice's cover, denoted  $C_1$ , is also in the JPEG format, the image is consequently double-compressed. Note that the setup is equivalent to classical (lossless) steganography if the platform does not recompress the uploaded image. In the following, we consider that the platform does compress the uploaded image.

We assume that Alice knows both the coding scheme and the coding parameters used by the platform. Practically, this can be done by inspecting the uploaded-downloaded images. The JPEG quantization matrix is public, and the coding scheme can often be identified by comparing the uploaded/downloaded image with the outputs of different coders.

Note that this setup follows the Kerckhoffs' principle, which states that anything not related to the secrecy of the application (here, the fact that a payload is potentially transmitted to Bob) should be considered public. Within this setup, the steganalyst Eve has access to the platform. She can also download images to try to differentiate an uploaded cover content (denoted  $C_2$ ) from an uploaded stego content ( $S_2$ ).

In order to minimize the difference between the uploaded image (respectively  $C_1$  or  $S_1$ ) and the downloaded image (respectively  $C_2$  or  $S_2$ ), we assume that the uploaded image is already coded with the same coding parameters than the downloaded image. Additionally, we assume that JPEG compression is the only process done during the upload on the platform, which means that the uploaded image is already resized correctly in order to prevent any resizing operation. This assumption is rather practical since it is usually the case on many platforms such as Facebook, WhatsApp, and Flickr [16], [17]...

### C. JPEG Coding Setup

Firstly, we recall the main features of the JPEG coding scheme. Without loss of generality, we assume that the original image is coded as greyscale. Still, the same methodology regarding the embedding mechanisms described in Sections III and IV can be applied on color channels, with or without subsampling.

- The original image is first decomposed into disjoint blocks of size  $8 \times 8$  pixels.
- Each block is then transformed into 64 DCT coefficients using the specific DCT type-II transform.
- Each coefficient is then quantized according to a quantization matrix specific to the coding algorithm and each DCT mode.

Note that there is a specific relation between the JPEG quality factor QF and the quantization matrix, but depending on the implementation of the coder, this relation can be different. For example, the Libjpeg library<sup>1</sup> use the classical relationship proposed by the standard (see [18], Section IV). On the contrary, the mozjpeg library<sup>2</sup> uses *ad hoc* quantization tables.

- For each block, the coefficients are scanned using a zigzag order.
- Depending on the coding scheme, the lossless entropic coding scheme can be different: the quantized coefficients are either directly coded using Run Length Coding and Huffman Coding, or a rate-distortion optimization procedure is applied to change the magnitude of several coefficients and to increase the coding rate.

Note that in the first case, the coefficients and blocks are independently coded, but in the second case, there is an interplay between the possible coefficient values and the length of the produced code. The potential use of the rate-distortion procedure depends on the implementation. For example, the Libjpeg library does not implement by default any rate-distortion procedure, but the mozjpeg library implements by default a Viterbi algorithm relying on a trellis.

<sup>1</sup><http://libjpeg.sourceforge.net>

<sup>2</sup><https://github.com/mozilla/mozjpeg>

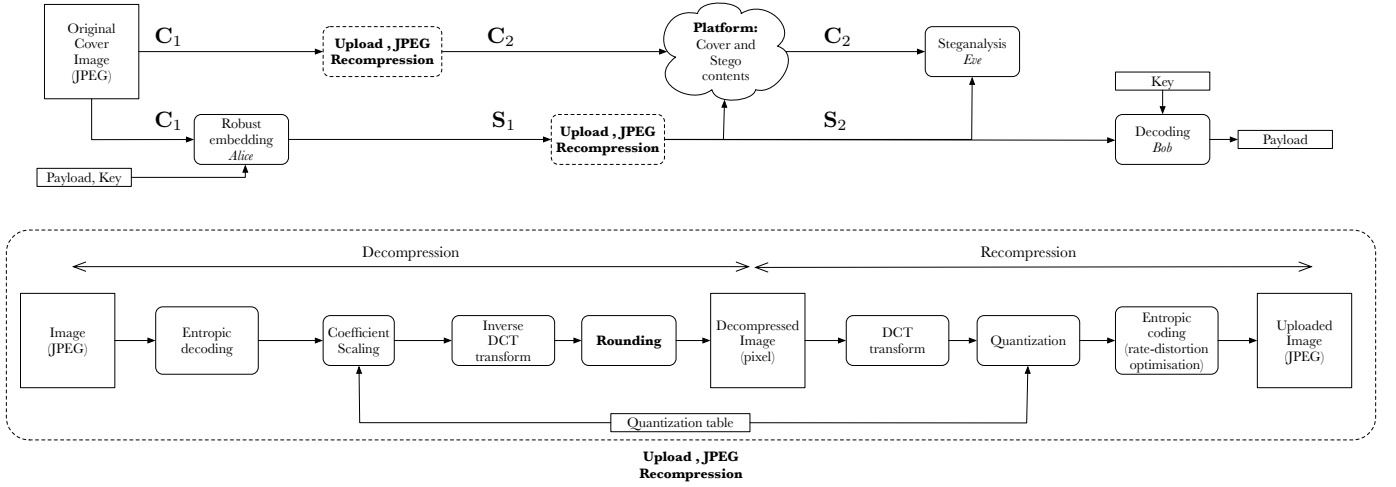


Fig. 1. Considered setups for robust steganography after JPEG compression: the top diagram represents the whole chain of processes and the different players (Alice, Bob, and Eve), see also Section II-B. The bottom diagram depicts the different operations involved in the uploading process, see also Section II-C.

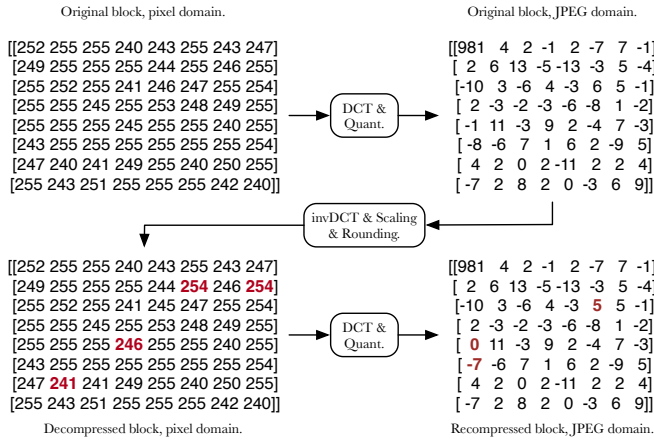


Fig. 2. Example of DCT coefficient changes after decompression and recompression (QF = 100). Changes in the pixel or JPEG domain are displayed in bold and dark red.

The upload of a JPEG image on the platform consists in decompressing and then recompressing the image (see Fig. 1, bottom). Before recompression, the JPEG image is decoded by first performing entropic decoding, coefficient scaling according to the quantization matrix, and inverse DCT transform. This is a lossy process because once decompressed, the pixel values are rounded to integer values between 0 and 255. This rounding operation in the pixel domain can modify a fraction of the DCT coefficients after recompression. Such an effect will be particularly significant (but not only) on blocks containing pixels initially clipped to 255 since, after decompression, the clipping may change the magnitude of DCT coefficients (see example depicted in Fig. 2).

This paper aims to propose a steganographic scheme that is robust to such a process.

### III. ROBUST EMBEDDING

#### A. Overview of the Embedding Algorithm

This section presents the robust embedding strategy. For better readability, we outline the general idea of the embedding scheme and only then describe the details of every mechanism involved.

First, we define a robust coefficient and how to extract the set of robust coefficients. Since one embedding change can potentially affect the robustness of many DCT coefficients from the same  $8 \times 8$  block, we divide the image into 64 non-overlapping lattices (one per DCT mode) and perform the embedding iteratively on every lattice separately. We assume for simplicity that every  $8 \times 8$  block is coded independently during the JPEG compression (we shall see in Section V the impact of this assumption when it is not the case).

Then, we show how to use the robustness of the coefficients during embedding. And finally, we look at how much payload shall be embedded in each of the 64 lattices.

The scheme of the embedding procedure is shown in Fig. 3.

#### B. Robustness

For ease of understanding, we introduce several definitions.

**Definition III.1** (Processed modes). Given  $k$ -th DCT mode (with a pre-defined ordering of modes),  $k \in \{1, \dots, 64\}$ , denote  $\mathcal{P}_k = \{1, \dots, k-1\}$ ,  $\mathcal{P}_1 = \emptyset$  the set of all modes that have already been processed by the algorithm.

**Definition III.2** (Pseudo-stego). The  $k$ -th pseudo-stego is the cover image with already embedded lattices from  $\mathcal{P}_k$ .

We will describe the process for a single  $8 \times 8$  block of single-compressed DCT coefficients of the  $k$ -th pseudo-stego  $\mathbf{c} = \{c_n\}_{n=1}^{64} \in \mathbb{Z}^{64}$ . Let  $i_n \in \mathbb{Z}^{64}$  be a vector containing  $i \in \mathbb{Z}$  at  $n$ -th coordinate and zeros elsewhere. Let  $R(\mathbf{c}, i_n) \in \mathbb{Z}^{64}$  denote the recompressed DCT coefficients of  $(\mathbf{c} + i_n)$ .

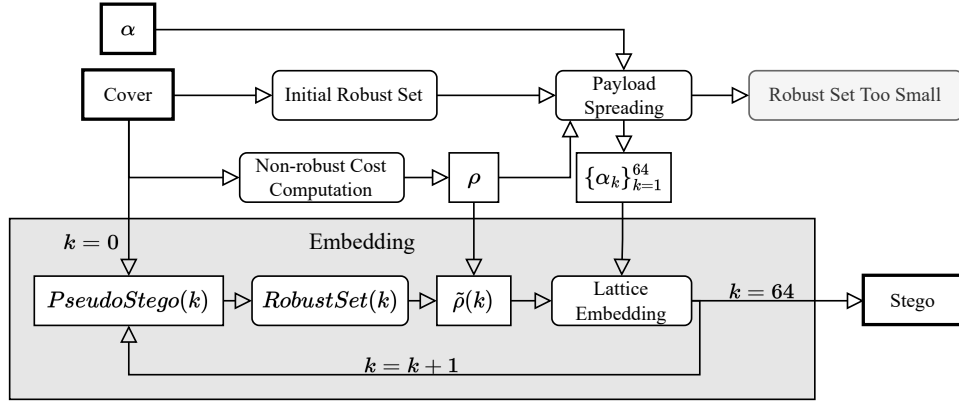


Fig. 3. Main steps of the embedding algorithm.

**Definition III.3** (Robust coefficient). We say a coefficient  $c_k$  is robust towards an embedding change  $i \in \{-1, 1\}$ , if during recompression it:

(R1): Does not change processed modes:

$$\forall l \in \mathcal{P}_k : R(\mathbf{c}, i_k)_l = R(\mathbf{c}, \mathbf{0})_l.$$

(R2): Preserves a change by  $i$ :

$$R(\mathbf{c}, i_k)_k = c_k + i.$$

(R3): Preserves no change:

$$R(\mathbf{c}, \mathbf{0})_k = c_k.$$

The sets of all robust coefficients towards  $+1$  and  $-1$  are denoted  $\mathcal{R}_k^+$  and  $\mathcal{R}_k^-$  respectively.

If a coefficient does not belong to a robust set, we say it is non-robust. The set of all non-robust coefficients is denoted  $\mathcal{R}_k^0$ .

Note that without (R1), embedding in the  $k$ -th lattice would destroy the message encoded in a lattice  $l \in \mathcal{P}_k$ , which would make the secret message unreadable.

(R2) states that the embedding change needs to survive the recompression.

(R3) gives us a choice during the embedding, whether to change the coefficient or not. We want to point out that a coefficient can belong to both sets  $\mathcal{R}_k^+$  and  $\mathcal{R}_k^-$ .

We illustrate these conditions graphically with a  $3 \times 3$  DCT block (for the sake of simplicity) in Fig. 4.

From the construction of the robust sets, the non-robust coefficients are coefficients  $c_k$ , such that either  $R(\mathbf{c}, \mathbf{0})_k \neq c_k$ , or  $R(\mathbf{c}, i_k)_k \neq c_k + i$ ,  $i \in \{-1, 1\}$ . In either case, it is essential to note that even though we cannot have control over the recompressed coefficient, we can compute its value  $R(\mathbf{c}, \mathbf{0})_k$ . We can see that this was, in fact, the case for one the already processed mode (0,1) in Fig. 4: its value changed from 3 to 2, but it does not prevent us from correctly embedding. For practical implementation with STCs, we perform standard embedding on the robust sets (with their possible embedding values) and do not change the non-robust set. This is done by setting their corresponding embedding costs to wet costs. Since we do have access to  $R(\mathbf{c}, \mathbf{0})$ , we are still able to encode

the message in the trellis. Section IV explains the embedding mechanism in further detail.

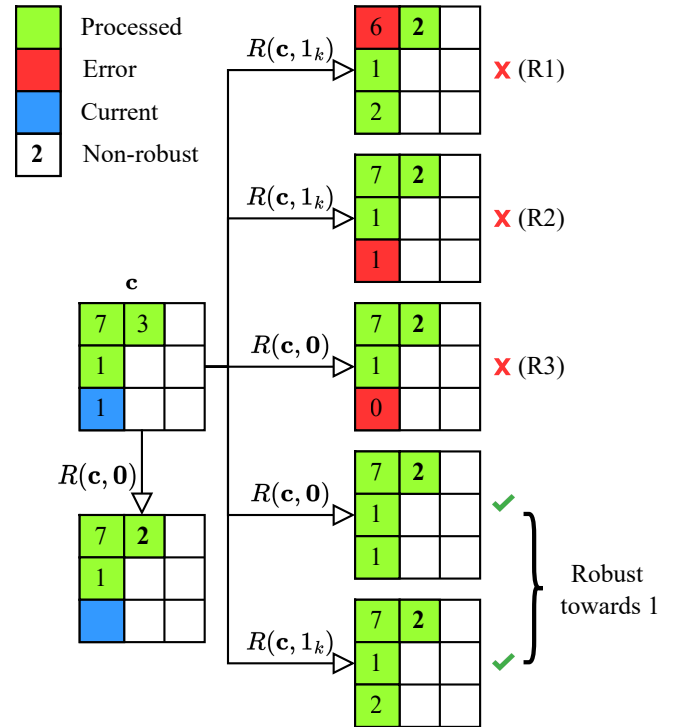


Fig. 4. Mechanism for deciding robustness of a DCT coefficient. Left: DCT coefficients  $\mathbf{c}$  and their recompressed values, Right: Possible effects of recompression on the current and processed lattices. The first three situations, each associated to one condition R1, R2 or R3, assign the coefficient to a non-robust set. Only if the last two situations arise is the coefficient robust towards 1.

### C. Lattice Embedding

To embed a given lattice, we need to compute the robust costs. Let  $\rho^+, \rho^-$  denote the embedding costs (computed from a given steganographic algorithm) of changing a DCT coefficient  $c$  by  $+1$  or  $-1$ . The robust costs  $\tilde{\rho}^+, \tilde{\rho}^-$  are created by updating the original costs:

$$\begin{cases} \tilde{\rho}^\pm = \rho^\pm, & c \in \mathcal{R}^+ \cap \mathcal{R}^-, \\ \tilde{\rho}^- = \infty, & c \in \mathcal{R}^+, \\ \tilde{\rho}^+ = \infty, & c \in \mathcal{R}^-, \\ \tilde{\rho}^\pm = \infty, & c \in \mathcal{R}^0. \end{cases} \quad (1)$$

In other cases, we keep  $\tilde{\rho}^+ = \rho^+$  and  $\tilde{\rho}^- = \rho^-$ .

Let  $\alpha_k$  be the portion of the total payload we desire to embed in the  $k$ -th lattice. For practical embedding, we would provide the embedding costs and payload to STCs to perform the embedding. However, in this work, we simulate the optimal embedding. Therefore we find the optimal change rates:

$$\beta_k^\pm = \frac{e^{-\lambda \tilde{\rho}_k^\pm}}{1 + e^{-\lambda \tilde{\rho}_k^+} e^{-\lambda \tilde{\rho}_k^-}}, \quad (2)$$

where  $\lambda > 0$  is the Lagrange multiplier ensuring that we embed the desired payload

$$\sum_{n=1}^N H_3(\beta_n^+, \beta_n^-) = \alpha_k,$$

and  $H_3(\beta^+, \beta^-)$  is the ternary entropy function

$$H_3(\beta^+, \beta^-) = -(1 - \beta^+ - \beta^-) \log(1 - \beta^+ - \beta^-) - \beta^+ \log \beta^+ - \beta^- \log \beta^-.$$

Having the optimal change rates, the coefficients from this lattice are embedded. That concludes the embedding of the given lattice, and we move on to the next.

#### D. Payload Spreading

Since our proposed method embeds iteratively 64 non-overlapping lattices, we need to decide *a priori* what portion of the embedding payload is carried in every lattice. Therefore, we compute the so-called ‘‘Initial robust set’’ for every lattice – the robust set without any embedding change. Let  $\alpha$  denote the total payload in bits we want to embed. Having the robust sets  $\mathcal{R}^+, \mathcal{R}^-, \mathcal{R}^0$ , we update the embedding costs (Eq. (1)) and compute the optimal change rates (Eq. (2)) for the whole image. From these change rates, we compute the proportion of payload  $\alpha_k$  in every lattice:

$$\alpha_k = \sum_{n=1}^N H_3(\beta_{n,k}^+, \beta_{n,k}^-),$$

where  $\beta_{n,k}^\pm$  is the  $n$ -th change rate in the  $k$ -th lattice. At this stage, it is possible that we cannot communicate the desired payload because of the small size of the robust set. In such a situation, we have no choice but to use a different image or a smaller secret message.

We are also well aware that there could be another potential issue during actual embedding with this approach of spreading the payload among lattices. In particular, the robust set in the  $k$ -th lattice could be of a very different size after embedding the previous lattices. As a result, we would not have enough robust coefficients to use for embedding a prescribed payload  $\alpha_k$ . However, in practice, we observed that the size of robust sets in each lattice changes in a negligible way, see Fig. 7.

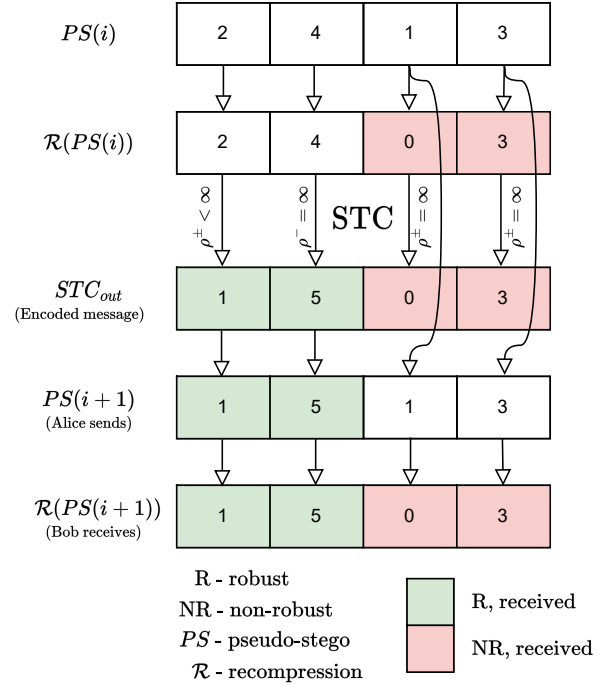


Fig. 5. Practical embedding of  $i$ -th lattice with Syndrom-Trellis Codes: Alice sends a bitstream which takes into account the recompression  $\mathcal{R}(\cdot)$  in order to be compliant with both the STC coding and decoding processes. The costs  $\rho$  are also chosen in order deal with non-robust modifications.

#### IV. PRACTICAL IMPLEMENTATION

In this section, we want to detail the technicalities necessary for actual embedding. First, JPEG compression is significantly impacted by the compressor. We consider three different JPEG compressors in this work: ImageMagick’s `convert`, `mozjpeg` (by default with rate-distortion optimization), and `mozjpeg` without optimization (-notrellis option). As mentioned earlier in Section II-C, the main difference between these compressors is the quantization tables used. Specifically, `mozjpeg` uses stronger quantization (bigger quantization steps) than `convert`. This harsher quantization positively affects the robustness of an image. In Fig. 6, we show the average initial robust size over 10 images compressed with the three compressors across a range of quality factors and with the random scanning strategy (see Section IV-A for more details about scanning strategies). We can see that for quality factors above 80, the images compressed with `convert` have a smaller robust set than those compressed with `mozjpeg` without the rate-distortion optimization. This is especially true around quality factor 90, where `convert` has a sudden drop in the robust set size. Strangely enough, `convert`’s robust size jumps back 93% for qualities 91,92. Although we are not sure why exactly this phenomenon is happening, we are convinced it is related to the quantization tables because we are unaware of another substantial difference between the compressors. Additionally, we can notice that disabling `mozjpeg`’s rate-distortion optimization increases the robust set size, mainly for qualities below 95.

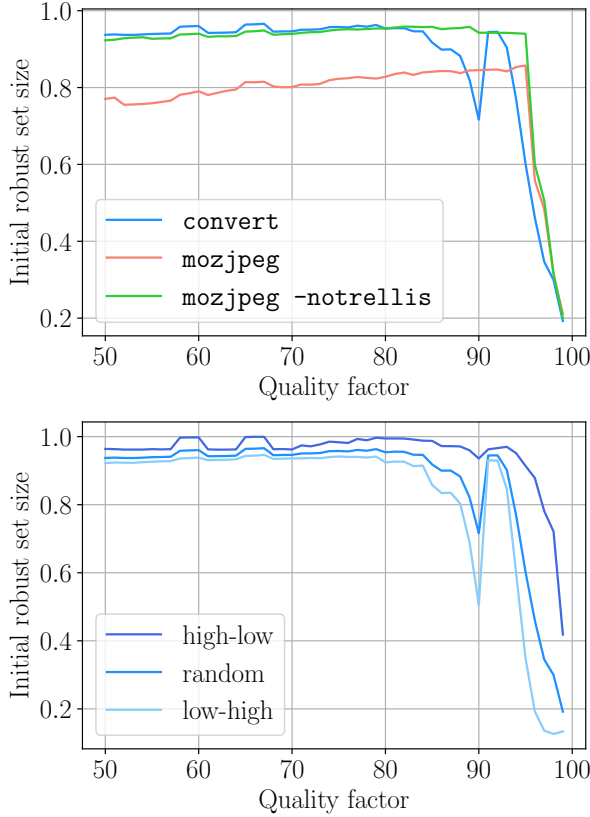


Fig. 6. Relative robust set size average over 10 cover images. Top: Random scanning strategy, bottom: `convert`

### A. Scanning Strategies

Secondly, we can notice that in the definition of *Processed modes*, we assumed a given ordering of DCT modes. We consider three natural scanning strategies:

- 1) Low-High: Scan modes in a zig-zag manner from low to high-frequency modes (as done in JPEG),
- 2) High-Low: Reverse the order of Low-High, and
- 3) Random: Randomly assign ordering of modes in every  $8 \times 8$  block.<sup>3</sup>

We will see in Section V that these three strategies will affect the empirical security of the embedding scheme.

Next, a scanning strategy dictates the size of the robust set in every lattice. In Fig. 7, we show the relative size of the robust set across all 64 lattices. The top two plots show the Low-High and High-Low scanning strategies for an image without saturated pixels, while the bottom plots show the Random scanning strategy for a non-saturated and a greatly saturated image. We can make several interesting observations from this figure. Robustness at QF 95 is generally smaller than for QF 75. This is to be expected, as bigger quantization steps (lower quality) provide more robustness against recompression. Similarly, since `mozjpeg`'s quantization steps are mostly bigger than those of `convert`, `mozjpeg` yields on average better robustness. We observe that the Random scan

<sup>3</sup>The pseudorandom key used for generating the permutations can be a part of the secret key.

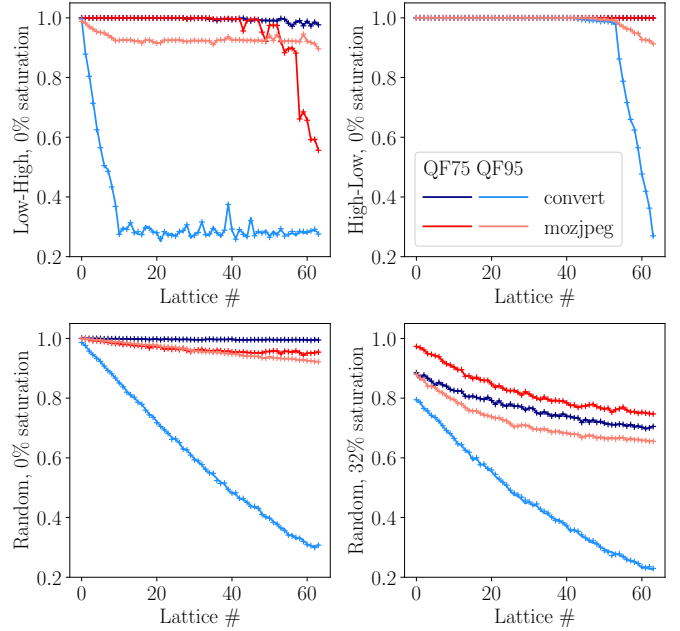


Fig. 7. Proportion of robust coefficients in every lattice during embedding. The solid line corresponds to a cover image (Initial robust set), while the crosses mark a stego image embedded with 0.8 bpnzAC. The first three figures are from a single BOSSBase image of size  $512 \times 512$  without any saturated pixels across three scanning strategies. The last figure shows the robustness of an image with 32% of its pixels saturated and random scan.

linearly decreases the robustness as we proceed through the lattices. It is important to realize that in the Random strategy, one lattice does not correspond to a DCT mode, as every block is scanned in a different random order. This ensures a relatively equal payload across all lattices, which allows us to skip the computation of the Initial robust set. In contrast, the first two scanning strategies assign one lattice per DCT mode, and it can be seen (especially for QF 95, `convert`) that most of the payload is carried in the low-frequency modes because their robustness decreases drastically. Finally, the saturation of pixels reduces the robustness due to the clipping of pixels into the dynamic range  $[0, 255]$  during recompression. During our experiments, all non-saturated images exhibit a similar trend, while robustness tends to decrease with increasing saturated area. Interestingly, we can also notice that the size of the Initial robust set in every lattice is not very different from the robust set of an image embedded with 0.8 bpnzAC. This justifies our payload allocation based on the Initial robust set (see Section III-D). If it were not the case, there would be a risk of having a lattice with a robust set that is too small for the desired payload.

### B. Syndrome-Trellis Coding

Lastly, we explain how to use the proposed methodology for practical embedding with Syndrome-Trellis Codes (STC). Fig. 5 shows Alice's action on a single lattice. Given  $i$ -th pseudo-stego, she will take the  $i$ -th lattice as a vector and inspect its recompressed values to assess the coefficients' robustness. She will then perform embedding on the recompressed lattice according to Section III-C. However, she cannot



simply send the output of the coding mechanism because the channel's recompression can potentially change the non-robust coefficients, which would prevent Bob from reading the secret message. Instead, Alice puts the original non-robust coefficients (before recompression) back into the lattice, which yields the  $(i+1)$ -th pseudo-stego. This way, it is ensured that after the recompression, Bob will be able to decode the secret message.

## V. RESULTS

The goal of this section is to benchmark the different characteristics of the proposed scheme within the framework of robust steganography. The considered setup will be the same as the one depicted in Fig. 1 and recalled in section II-B, *i.e.* the steganographer will embed its payload on a single-compressed image and submit it on the platform that will compress the stego image. On the other side, the steganalyst will observe contents that are published on the platform, *i.e.* contents which are double-compressed, either in their cover or stego version. The lossy coding algorithm and used parameters by the steganographer and the platform will be identical. The considered figures of merit are the following:

- The *practical security* of the robust scheme for different scanning strategies and JPEG compressors. It is also important to compare it w.r.t. the naive embedding which is not robust but maximizes the security and can be considered as a baseline.
- The *embedding success rate*, *i.e.* the probability to be able to embed the prescribed payload. The size of the robust set being limited, for high-quality factors, the robust set may be too small on several images.
- The *impact of the compressor*, such as `mozjpeg` or `convert`, which can use specific quantization matrices or can optimize the rate-distortion trade-off and which can change quantization values before applying Huffman coding.

These different features are evaluated using a classical steganography/steganalysis setup:

- Images from BOSSBase [19] in greyscale format are used as a source of covers. Images in the pixel/PGM format are used as pre-covers and then compressed with the appropriate compressor.
- Regarding steganography, UERD [2] is chosen as the embedding scheme because it offers a good tradeoff between complexity and practical security. Different payload sizes ranging from 0.1 bpnzAC to 0.4 bpnzAC are adopted.
- Regarding steganalysis, DCTR features [20] are combined with the regularized linear classifier [21]. 5000 pairs of images are used for training, and 5000 pairs for testing.
- The classical probability of error  $P_e$  minimizing the sum of false positive and false negative rates during training is reported as a measure of practical security.

Different quality factors, ranging from 50 to 100, are reported to analyze the evolution of the mentioned features w.r.t.

JPEG quantization. Note, however, that there is a substantial discrepancy between the quantization matrices used by `libjpeg/convert` and `mozjpeg`, the quantization steps used by `mozjpeg` being always greater or equal to the quantization steps used by `convert`.

Note also that, except when explicitly mentioned in the case of rate-distortion optimization, the proposed scheme is errorless. Consequently, no error-correcting codes need to be used, and no error transmission probability needs to be reported.

### A. Practical security

Fig. 8, Fig. 9 and Fig.10 present respectively the detection error  $P_e$  for respectively `convert`, `mozjpeg` without (option `-notrellis` added) and `mozjpeg` with the rate-distortion trade-off.

Several remarks can be drawn from this extensive set of experiments.

a) *On the impact of the scan strategy:* The strategy of randomly picking the DCT modes for each lattice offers a gain of practical security w.r.t. to scans starting with low frequencies or high frequencies except for very high-quality factors (*i.e.*  $\geq 95$ ). For quality factors below 85, the gain associated with the random scan is between 2 and 5% w.r.t. the other scans. However, one can choose the scan starting with low-frequency modes for high-quality factors. It is also interesting to notice that starting with low frequencies is, on average, a better strategy than scanning the high frequencies first, even if the size of the robust set is far larger with the second option (see Fig. 7). We can see that there is a tradeoff between the size of the robust set and the modes it considers as robust.

On one side, the high-frequency modes are more robust since they are associated with bigger, hence more conservative, quantization steps; on the other side, they are more detectable.

Note also that, on average, the random-scan strategy has to be preferred because of its higher security and its possibility to spread the payload without first computing the robust set (see section IV).

b) *On the gap between robust and non robust embedding:* When comparing with the most favorable embedding strategy, we can observe that, at 0.1 bpnzAC, the gap is very small (*i.e.* below 3% in terms of detection error) but becomes substantial (*i.e.* reaching more than 10% for few quality factors) for larger embedding rates and high-quality factors. This is not surprising since we have seen in Section IV that the size of the robust set tends to decrease w.r.t. the quality factor, which means that the embedding algorithm has to perform more embedding changes. Indeed, for the same payload size, the number of embedding changes decreases w.r.t. the number of changeable coefficients. The larger detectability is also due to the fact that the non-robust coefficient initially associated with small embedding costs in a non-robust setting cannot be modified anymore with the proposed scheme. They are lost for embedding.

c) *On the impact of the quality factor:* For the `convert` coder, we can notice a "bump" for quality factors between 90

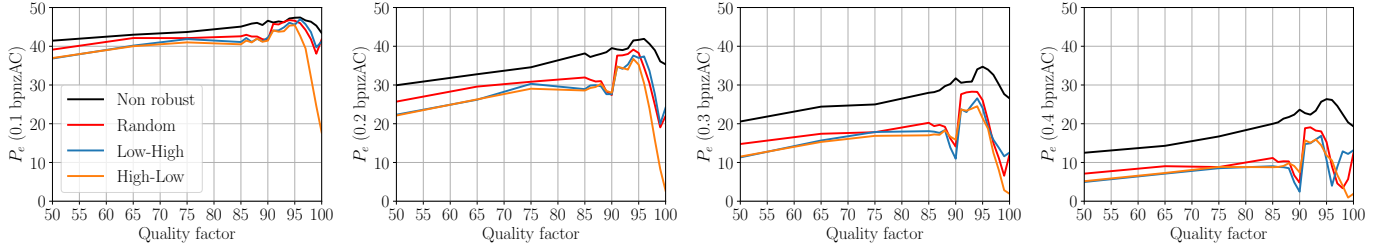


Fig. 8. Detection errors with `convert`.

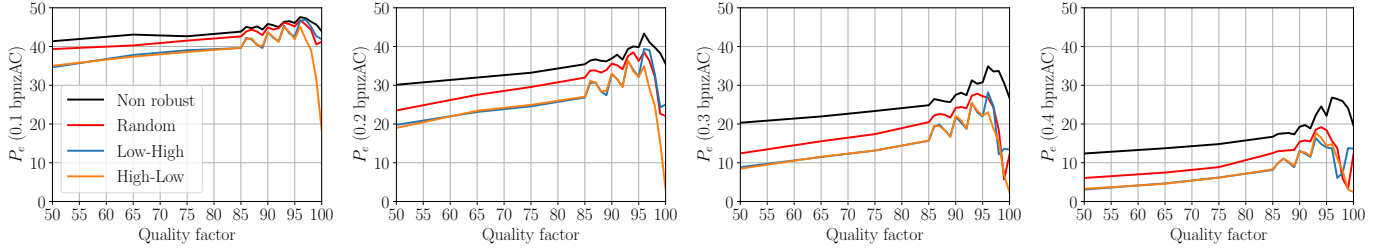


Fig. 9. Detection errors with `mozjpeg` without rate-distortion optimization.

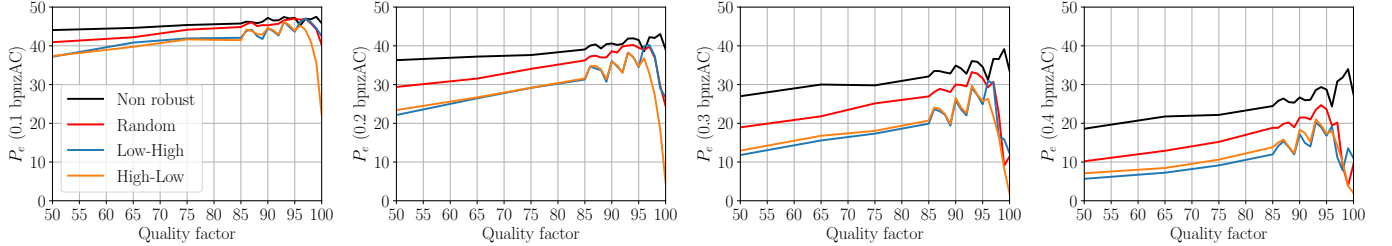


Fig. 10. Detection errors with `mozjpeg` with rate-distortion optimization.

and 100, which is associated with an increase of detectability w.r.t. the non-robust scheme. For the `mozjpeg` coder, we can also observe oscillations of the overall detectability. We hypothesize that these two phenomena are due to the interplay between DCT modes quantized with specific steps. From Fig. 6, we can observe that the oscillations in terms of detectability are on par with the ones coming from the size of the robust sets. Note also that part of the non-monotony of the detectability is also due to the quantization tables only and was already observed for plain JPEG steganography [22].

*d) On the impact of the coder:* If, as reported above, the different quantization tables used by the two coders are associated with different detectabilities, we can also notice that whenever the `mozjpeg` coder uses rate-distortion optimization, the practical detectability is smaller. If we noticed that the payload size is smaller (the number of 0s increases by about 10% after the optimization), it is probably not the only reason since the same decrease of 0s is observed between `convert` and `mozjpeg` without optimization.

We hypothesize that the produced cover images with optimization are also more “secure” sources since they have less isolated non-zero modes due to the optimization process.

## B. Embedding success rate

Because the size of the robust set can be limited, the maximum embedding capacity for ternary embedding can be smaller than  $\log_2(3) \approx 1.58$  bit per coefficient. If the prescribed embedding rate (chosen to be in bpnzAC) is larger than the maximum achievable rate, we consequently report an embedding failure. Table I reports the embedding success rate computed on the BOSSBase database for the different coders, different scanning strategies, embedding rates ranging from 0.1 bpnzAC to 0.4 bpnzAC, and different quantization factors. We can draw several conclusions:

- For  $QF \leq 94$ , the embedding success rate reaches 100%, but the higher the quality factor, the less robust the embedding is. This is due to the fact that, in this range of quality factors, the size of the robust set decreases.
- The Low-High scan is less robust than the Random scan, which is less robust than the High-Low scan. This is coherent with the size of the robust sets, which follow the same trend (the robust set associated with the Low-High is smaller than the robust set associated with the Random scan, which is smaller than the one associated with the High-Low) plotted in Fig. 6
- The `mozjpeg` coder with rate-distortion optimization is more robust than the same coder without optimization,



which is, in turn, more robust than the `convert` coder. Again, this is coherent with the hierarchy on the robust set size, plotted in Fig. 6.

### C. Impact of rate-distortion strategies

This last experiment investigates to what extent the rate-distortion strategy, which is used by the `mozjpeg` coder to decrease the file size by changing DCT coefficients values and to decrease their associated Huffman code length, is detrimental to the robustness of the scheme. This is conducted out of curiosity since we know in advance that the proposed scheme is not robust to change of coefficient after quantization. Fig. 11 shows the ratio of images that can convey the payload when this option is activated.

Here we can see two behaviors:

- 1) For quality factors  $\leq 95$ , starting with low-frequency coefficients increases the correct extraction rate significantly. For quality factors  $> 95$ , starting with the High-frequency coefficient offers the best extraction rate. Moreover, there is an overall drop in extraction rate for quality factors  $> 95$ , which is caused by reduced robust set size (see Fig. 6).
- 2) The larger the embedding rate, the smaller the number of images having a correct extraction. However, we can note that in a favorable setting (Low to High scan and QF below 95 at 0.1 bpzAC), the ratio of the correctly extracted payload is larger than 60%.

## VI. CONCLUSIONS AND PERSPECTIVES

In this work, we introduced a methodology for JPEG steganography robust against subsequent recompression. Although the JPEG compressor has to be assumed known, it does not present any obstacles because, in a typical channel, a social media, we can easily access the compressor. First, we introduced the notion of the robustness of a DCT coefficient. We showed that this could be done by dividing the image into 64 non-overlapping lattices and performing 64 consecutive recompressions (associated with  $\pm 1$  modifications) of an image, one per lattice. We introduced three ordering of the lattices: Low to High, High to Low, and Random. We showed that these three strategies offer different robust sets. Then we combined the coefficients' robustness with steganographic costs from a non-robust stego algorithm in a straightforward way to robustify the algorithm. Additionally, it was shown how this could be done in a practical setting with Syndrome-Trellis Codes.

In the last part of the paper, we evaluate the security of our method with machine-learning steganalysis. We observe that the security is affected by everything in the system: Quality Factor, compressor, and the scanning strategy of the lattices. We link the differences in security to different sizes of the robust sets. Moreover, we can observe security loss compared to the non-robust version of the stego algorithm, which is expected because many coefficients with small embedding costs will not be usable for robust embedding. Lastly, unlike any of the preceding works on robust steganography, our method

is truly errorless, giving us guarantees on the readability of the embedded secret message. The only exception to this is `mozjpeg` which allows rate-distortion optimization. On the other hand, we have seen that, if successfully embedded, the rate-distortion optimization increases the security of the underlying scheme.

In the future, we plan to derive theoretical bounds on the embedding capacity in the noisy recompression channel. The source code of the proposed robust embedding will be made available from <https://janbutora.github.io/downloads/> upon acceptance of this paper.

## REFERENCES

- [1] V. Holub, J. Fridrich, and T. Denemark, "Universal distortion function for steganography in an arbitrary domain," *EURASIP Journal on Information Security*, vol. 2014, no. 1, pp. 1–13, 2014.
- [2] L. Guo, J. Ni, W. Su, C. Tang, and Y.-Q. Shi, "Using statistical image model for jpeg steganography: Uniform embedding revisited," *IEEE Transactions on Information Forensics and Security*, vol. 10, no. 12, pp. 2669–2680, 2015.
- [3] Q. Giboulot, R. Cogranne, and P. Bas, "Detectability-based JPEG steganography modeling the processing pipeline: the noise-content trade-off," *IEEE Transactions on Information Forensics and Security*, vol. 16, pp. 2202–2217, Jan. 2021. [Online]. Available: <https://hal.archives-ouvertes.fr/hal-03096658>
- [4] P. Bas, F. Teddy, F. Cayre, G. Doërr, and B. Mathon, *Watermarking Security: Fundamentals, Secure Design and Attacks*. Springer, Jan. 2016.
- [5] F. Cayre and P. Bas, "Kerckhoffs-based embedding security classes for WOA data-hiding," *IEEE Transactions on Information Forensics and Security*, vol. 3, no. 1, March 2008.
- [6] C. Kin-Cleaves and A. D. Ker, "Adaptive steganography in the noisy channel with dual-syndrome trellis codes," in *2018 IEEE International Workshop on Information Forensics and Security (WIFS)*. IEEE, 2018, pp. 1–7.
- [7] T. Filler, J. Judas, and J. Fridrich, "Minimizing additive distortion in steganography using syndrome-trellis codes," *Information Forensics and Security, IEEE Transactions on*, vol. 6, no. 3, pp. 920–935, 2011.
- [8] Y. Zhang, X. Luo, C. Yang, D. Ye, and F. Liu, "A framework of adaptive steganography resisting jpeg compression and detection," *Security and Communication Networks*, vol. 9, no. 15, pp. 2957–2971, 2016.
- [9] W. Luo, G. L. Heileman, and C. E. Pizano, "Fast and robust watermarking of jpeg files," in *Proceedings Fifth IEEE Southwest Symposium on Image Analysis and Interpretation*. IEEE, 2002, pp. 158–162.
- [10] T. Qiao, S. Wang, X. Luo, and Z. Zhu, "Robust steganography resisting jpeg compression by improving selection of cover element," *Signal Processing*, vol. 183, p. 108048, 2021.
- [11] J. Tao, S. Li, X. Zhang, and Z. Wang, "Towards robust image steganography," *IEEE Transactions on Circuits and Systems for Video Technology*, vol. 29, no. 2, pp. 594–600, 2018.
- [12] W. Lu, J. Zhang, X. Zhao, W. Zhang, and J. Huang, "Secure robust jpeg steganography based on autoencoder with adaptive bch encoding," *IEEE Transactions on Circuits and Systems for Video Technology*, 2020.
- [13] Z. Zhao, Q. Guan, H. Zhang, and X. Zhao, "Improving the robustness of adaptive steganographic algorithms based on transport channel matching," *IEEE Transactions on Information Forensics and Security*, vol. 14, no. 7, pp. 1843–1856, 2018.
- [14] Y. Zhang, X. Luo, J. Wang, C. Yang, and F. Liu, "A robust image steganography method resistant to scaling and detection," *Journal of Internet Technology*, vol. 19, no. 2, pp. 607–618, 2018.
- [15] L. Zhu, X. Luo, Y. Zhang, C. Yang, and F. Liu, "Inverse interpolation and its application in robust image steganography," *IEEE Transactions on Circuits and Systems for Video Technology*, vol. 32, no. 6, pp. 4052–4064, 2021.
- [16] A. Castiglione, G. Cattaneo, and A. De Santis, "A forensic analysis of images on online social networks," in *2011 third international conference on intelligent networking and collaborative systems*. IEEE, 2011, pp. 679–684.
- [17] R. Caldelli, R. Becarelli, and I. Amerini, "Image origin classification based on social network provenance," *IEEE Transactions on Information Forensics and Security*, vol. 12, no. 6, pp. 1299–1308, 2017.

Emb. rate (bpnzAC)	Scan	Coder	94	95	96	97	98	99	100
0.1	all	all	100	100	100	100	100	100	100
0.2	Random and High-Low	all	100	100	100	100	100	100	100
0.2	Low-High	convert	100	100	99.98	99.72	94.53	89.95	99.97
0.2	Low-High	moz jpeg, no optim	100	100	100	99.98	98.22	88.25	99.89
0.2	Low-High	moz jpeg, optim	100	100	99.98	99.98	99.44	92.91	99.92
0.3	Low-High	convert	100	99.98	99.29	71.87	44.04	25.64	30.45
0.3	High-Low	convert	100	100	100	100	100	100	20.08
0.3	Random	convert	100	100	100	100	100	87.72	27.71
0.3	Low-High	moz jpeg, no optim	100	100	99.98	99.88	58.09	28.99	30.24
0.3	High-Low	moz jpeg, no optim	100	100	100	100	100	100	19.93
0.3	Random	moz jpeg, no optim	100	100	100	100	99.99	98.31	27.55
0.3	Low-High	moz jpeg, optim	100	100	99.96	99.89	72.74	45.64	49.37
0.3	High-Low	moz jpeg, optim	100	100	100	100	100	100	63.5
0.3	Random	moz jpeg, optim	100	100	100	100	99.98	99.39	57.82
0.4	Low-High	convert	100	99.95	84.53	34.9	18.8	10.18	7.96
0.4	High-Low	convert	100	100	100	100	100	100	4.82
0.4	Random	convert	100	100	100	100	99.98	33.12	6.65
0.4	Low-High	moz jpeg, no optim	100	100	99.94	96.71	23.03	11.85	7.89
0.4	High-Low	moz jpeg, no optim	100	100	100	100	100	100	4.83
0.4	Random	moz jpeg, no optim	100	100	100	100	99.97	59.59	6.63
0.4	Low-High	moz jpeg, optim	100	100	99.92	98.07	39.73	22.34	19.97
0.4	High-Low	moz jpeg, optim	100	100	100	100	100	100	34.83
0.4	Random	moz jpeg, optim	100	100	100	99.98	99.97	76.0	26.61

TABLE I

EMBEDDING SUCCESS RATES FOR DIFFERENT JPEG QUALITY FACTORS (IN %) WITH CONVERT AND MOZ JPEG WITH AND WITHOUT RATE-DISTORTION OPTIMIZATION.

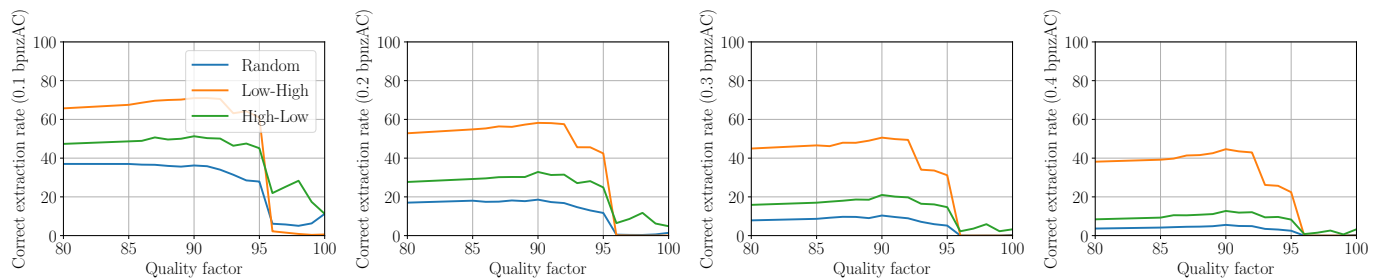


Fig. 11. Correct extraction rate (in %) for moz jpeg with rate-distortion optimization for different embedding rates.

- [18] J. Butora and J. Fridrich, "Revisiting perturbed quantization," in *Proceedings of the 2021 ACM Workshop on Information Hiding and Multimedia Security*, 2021, pp. 125–136.
- [19] P. Bas, T. Pevny, and T. Filler, "Bossbase," <http://exile.felk.cvut.cz/boss>, May 2011.
- [20] V. Holub and J. Fridrich, "Low-complexity features for jpeg steganalysis using undecimated dct," *IEEE Transactions on Information Forensics and Security*, vol. 10, no. 2, pp. 219–228, 2015.
- [21] R. Cogranne, V. Sedighi, J. Fridrich, and T. Pevný, "Is ensemble classifier needed for steganalysis in high-dimensional feature spaces?" in *Information Forensics and Security (WIFS), 2015 IEEE International Workshop on*. IEEE, 2015, pp. 1–6.
- [22] J. Butora and J. Fridrich, "Effect of jpeg quality on steganographic security," in *Proceedings of the ACM Workshop on Information Hiding and Multimedia Security*, 2019, pp. 47–56.